

VIBRATION CHARACTERISTICS, CHEMICAL BONDS AND WEAK INTERACTIONS OF 4- AND 5-HYDROXSALICYLIC ACID INVESTIGATED BY TERAHERTZ SPECTROSCOPY AND DENSITY FUNCTIONAL THEORY

Yuan Tang^{a,*}, Zhi Li^{a,b,*}, Yan Guo^b, Xianhua Yin^a, Shan Tu^c and Dapeng Zhang^a

^aGuangxi Key Laboratory of Automatic Detecting Technology and Instruments, School of Electronic Engineering and Automation, Guilin University of Electronic Technology, Guilin 541004, China

^bKey Laboratory of Unmanned Aerial Vehicle Telemetry, Guilin University of Aerospace Technology, Guilin 541004, China

^cGuangxi Key Laboratory of Nuclear Physics and Technology, Guangxi Normal University, Guilin 541004, China

Recebido em 10/01/2022; aceito em 18/03/2022; publicado na web em 19/04/2022

The terahertz (THz) absorption spectra of 4- and 5-hydroxysalicylic acid were measured by terahertz time-domain spectroscopy (THz-TDS) in the range of 0.4–2.8 THz. The unit cells of both were calculated by density functional theory (DFT), and the theoretical simulation and experimental data were basically in agreement. To further interpret the origin of the characteristic absorption peaks, vibration characteristics and interactions of the unit cell model were analyzed by using potential energy distribution (PED) and interaction region indicator (IRI) method. The analysis indicated that the absorption peaks of 4- and 5-hydroxysalicylic acid were mainly derived from the vibration mode of dihedral angle torsion, and were closely related to the hydrogen bonds. And the intermolecular weak interaction of both were mainly dominated in quantity by van der Waals interaction. The results show that this is an effective solution to identify isomers and explain the formation mechanism of characteristic absorption peaks by using THz-TDS and combining PED and IRI methods.

Keywords: THz-TDS; DFT; vibration characteristics; chemical bonds; weak interactions.

INTRODUCTION

4- and 5-hydroxysalicylic acid are isomers and they are derivatives of salicylic acid, but their properties and uses are different. 5-hydroxysalicylic acid is also called gentian acid, it is a polyhydroxy carboxylic acid. It belongs to the secondary product of salicylic acid through renal metabolism. In addition, it is also an important pharmaceutical intermediate. In the pharmaceutical industry, 5-hydroxysalicylic acid is often used as an antioxidant excipient. At the same time, it is also an antipyretic and analgesic.¹ 4-hydroxysalicylic acid has both chemical properties of resorcinol and salicylic acid. It is mainly used as dye and pharmaceutical intermediates.

The fine chemical and pharmaceutical industries need to focus on the safety and quality of synthetic intermediates, especially those with similar appearance but different physical and chemical properties. Therefore, an accurate, rapid and non-destructive method is needed to identify chemical intermediates with similar appearance but different physical and chemical properties. THz-TDS is based on femtosecond ultrafast laser technology to obtain the characteristic fingerprint spectrum of substances in THz band, and then can effectively study the characteristics of substances at low frequency.^{2,3} According to the investigation, the low-frequency vibration modes of many biological macromolecules are mostly caused by the collective vibration between molecules, the swing of intermolecular hydrogen bonds and the torsion of large official energy groups.⁴ When the sample is detected by terahertz wave, if the vibration or rotation frequency of the sample molecular structure is consistent with the terahertz frequency, resonance absorption will occur, and the formed absorption peak spectrum is unique.⁵ Compared with terahertz wave, Infrared and Raman spectroscopy are usually used to analyze the vibration modes of chemical bonds and functional groups, and their accuracy

is low for substances from the same category as their chemical bonds and functional groups are very similar. THz wave is just in the far-infrared band, which is extremely sensitive to intermolecular interaction and surrounding environment, and it has good penetration and special spectral characteristics, which can be used in contactless identification of substances.⁶ In addition, weak intermolecular interactions in crystals, such as hydrogen bond stretching and torsion, fall in the terahertz band, which makes THz-TDS an effective means to study weak intermolecular interactions. Based on THz-TDS, in 2005, Yamaguchi *et al.*⁷ measured the low-frequency THz absorption spectra of alanine chiral isomers and racemates by using THz-TDS. It was found that the absorption peak positions of alanine with different structures were significantly different. In 2012, Zheng *et al.*⁸ measured the absorption spectra of catechol, resorcinol and hydroquinone by using THz-TDS, and found that they had their own absorption peaks in the effective THz band.

Salicylic acid is an important organic synthetic raw material, which is widely used in medicine, pesticide, rubber, dye, food and flavor industries.⁹⁻¹¹ It has attracted many scholars at home and abroad to study its terahertz spectral characteristics, but there are few reports on the terahertz spectral characteristics of its hydroxyl derivatives. 4- and 5-hydroxysalicylic acid are the important pharmaceutical intermediates. And it has great significance to study the formation mechanism of its THz spectral absorption peaks for the research on the biochemical function of drugs and the synthesis and development of new drugs. Figure 1 shows the single-molecule model structures of 4- and 5-hydroxysalicylic acid.

EXPERIMENTAL

Experimental apparatus

The schematic diagram of the THz-TDS system (Z-3, produced by Zomega, USA) used in the experiment is shown in Figure 2.^{12,13}

*e-mail: cclizhi@guet.edu.cn

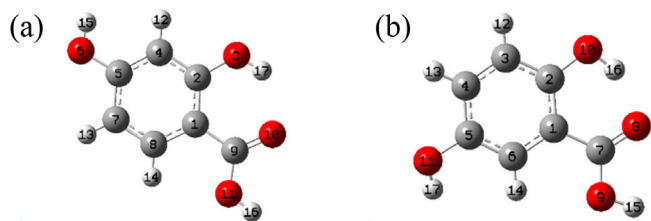


Figure 1. Monomolecular structures of the hydroxysalicylic acid isomers. (a) 4-hydroxysalicylic acid. (b) 5-hydroxysalicylic acid. Atomic elements in gray, white, and red represent carbon, hydrogen, and oxygen atoms, respectively

The repetition frequency is 82 MHz, the pulse duration is 100 fs, and the center wavelength is 780 nm. The system is mainly composed of four parts: ultrafast femtosecond fiber laser, THz radiation generator, THz radiation detection device and time delay control system. The femtosecond laser sends laser pulses through the half-wave plate (HWP) and is divided into two orthogonal pulses by the polarization beam splitter (PBS). The strong beam as the pump pulse passes through the optical delay system (Stage) and irradiates the GaAs crystal to generate THz pulses, which are collimated and focused to the measured sample carrying the scattering and absorption information of the sample; while the weak beam is used as the detection pulse. After multiple reflections, it is irradiated on high-resistance silicon (Si) through the polarizer P, and after reflection, it is incident on the detection crystal (ZnTe) collinearly with the THz wave carrying the sample information, and the terahertz wave detector is driven for measurement. The inter-delay control system is used to adjust the time delay of the two pulses to obtain the THz time-domain signal carrying the sample information, and then the Fourier transform is used to obtain the physical parameters such as the absorption coefficient and refractive index of the sample. The experiment is carried out at room temperature. In order to reduce the absorption of THz pulses by moisture, dry nitrogen must be filled into the closed THz light path to ensure that the relative humidity of the measurement environment is controlled below 2%.

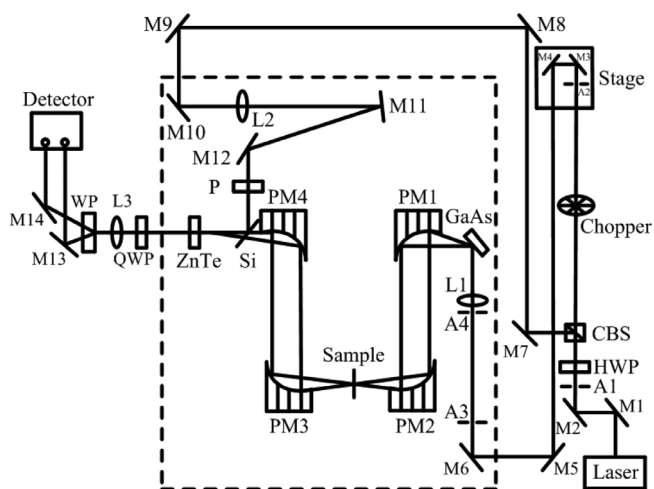


Figure 2. Schematic diagram of the THz-TDS system

Sample preparation

The experimental samples were purchased from Shanghai Macleans Biochemical Technology Co., Ltd., and the purity was 98%, which met the experimental requirements. The sample was placed in a vacuum constant temperature drying oven at 50 °C to dry for about 2 hours to remove residual moisture. The samples were respectively mixed with polyethylene powder (mass ratio 3:1), and

ground in a mortar. Then use the FW-4A tablet press (the pressure value is adjusted to 12 Mpa) to compress the samples into uniform sheets with a thickness of about 1.2 mm and a diameter of 13 mm.¹⁴

Data processing

The reference signal and sample signal obtained in the experiment are converted into the corresponding frequency domain signal by the fast Fourier transform (FFT). The absorbance, absorption coefficient, and refractive index are essential optical parameters that describe the macroscopic optical properties of the research object. These parameters can be obtained based on the optical parameter model proposed by Duvillaret and Dorney.^{15,16} The absorbance is used to process the experimental data. The absorbance represents the degree to which the THz wave is absorbed by the sample. It is a relative quantity and dimensionless. According to the description of the Fresnel formula, the absorbance $A(\omega)$ parameter can be obtained by the following formula.¹⁷

$$A(\omega) = \lg \left| \frac{E_{ref}(\omega)}{E_{sam}(\omega)} \right|^2 \quad (1)$$

where $E_{sam}(\omega)$ is the THz amplitude of the sample, $E_{ref}(\omega)$ is the THz amplitude of the reference, and ω is the circular frequency. The THz absorption spectra of 4- and 5-hydroxysalicylic acid were plotted via Origin software after the processing described above.

THEORETICAL METHODS

Density functional theory method

Density functional theory is a quantum mechanical method for studying multi-electron systems. It was proposed by Hohenberg and Kohn in 1964 on the theoretical basis of the Thomas-Fermi model of homogeneous electron gas.¹⁸ The main goal of density functional theory is to replace the wave function with electron density as a fundamental quantity. The crystal structure parameters and configurations of 4- and 5-hydroxysalicylic acid are from the Cambridge Crystallographic Data Center (CCDC).¹⁹ Considering the size and calculation accuracy of the system, the DFT theoretical calculation adopts the hybrid functional B3LYP, the basis set is 6-311G**, and the dispersion correction (DFT-D3) proposed by Grimme is added at the same time.²⁰ The unit cell structures of the samples were geometrically optimized, and the frequency of the stable molecular structures were calculated by using Gaussian 16 software.^{21,22}

PED method

PED is a method of decomposing the normal vibration mode, which can obtain the contribution ratio of each group to the normal vibration mode. It is easier to analyze the essential characteristics of the vibration mode and the dominant vibration mode type by comparing the contribution percentages. The contribution of the i -th valence-force coordinate in the k -th normal mode, the percent of Potential Energy Distribution, can be written as follows.²³

$$PED_{ki} = \frac{\sum_j F_{s,ij} L_{s,kj}^{-1} L_{s,ki}^{-1}}{\sum_{l,j} F_{s,lj} L_{s,kj}^{-1} L_{s,lj}^{-1}} \quad (2)$$

where F_s is the force constant matrix under internal coordinates, and L_s is the eigenvector matrix.

Interaction Region Indicator

The THz absorption spectrum of molecular crystals consists of lattice vibrations, and lattice vibrations are the products of intermolecular interactions unique to the unique three-dimensional arrangement inside the crystal. Therefore, further identification of the weakly interacting components in the system will help a more comprehensive understanding of spectral information. This paper uses the interaction region indicator (IRI) method to analyze and study weak interactions between molecules. In 2021, Lu *et al.*²⁴ proposed the interaction region indicator (IRI) method, which is an improvement on the currently popular RDG method.²⁵ The IRI method can clearly show the type, intensity and position of the intermolecular interaction in a picture through its iso-surface. The definition of the IRI function is particularly simple, as shown below:

$$IRI(\mathbf{r}) = \frac{|\nabla \rho(\mathbf{r})|}{[\rho(\mathbf{r})]^a} \quad (3)$$

where ∇ is the gradient operator, $\rho(r)$ is the electron density, and where a is an adjustable parameter, $a=1.1$ is adopted for standard definition of IRI. After the conventional quantum chemical calculation, the electron density and its gradient can be easily calculated according to the wave function information contained in the output file. In order to visually show the type of weak interaction, the $\text{sign}(\lambda_2)$ function needs to be introduced. $\text{Sign}(\lambda_2)$ is the symbol representing the second largest eigenvalue of the Hessian matrix of electron density. The $\text{sign}(\lambda_2)$ ρ function can be mapped to the IRI iso-surface through different colors to vividly show the nature of the interaction area revealed by IRI. As shown in Figure 3.

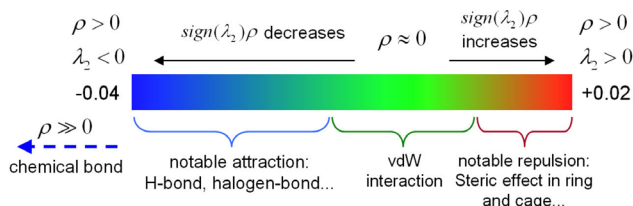


Figure 3. Standard coloring method and chemical explanation of $\text{sign}(\lambda_2)\rho$ on IRI iso-surfaces

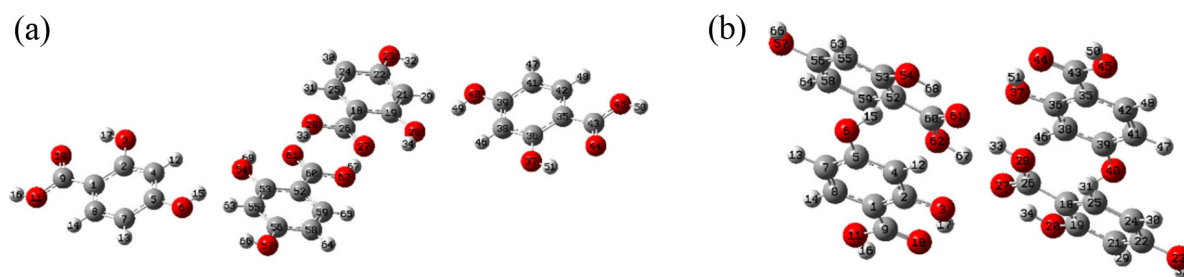


Figure 4. The unit cell structures of 4-hydroxysalicylic acid. (a) Before optimization. (b) After optimization

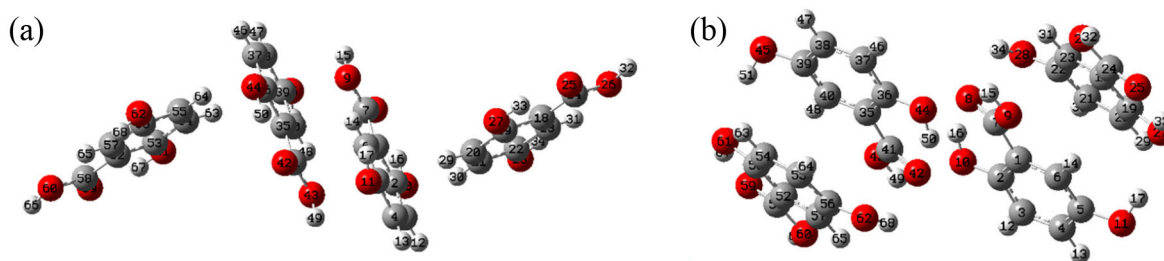


Figure 5. The unit cell structures of 5-hydroxysalicylic acid. (a) Before optimization. (b) After optimization

RESULTS AND DISCUSSION

Experimental and theoretical simulated spectra analysis

The unit cell of 4- and 5-hydroxysalicylic acid was theoretically calculated by using Gaussian 16 software combined with DFT-D3 method. One unit cell of both samples includes four molecules. Figure 4 and Figure 5 show that the unit cell structures before and after optimization for the two samples. Obviously, the molecules are closer together for the optimized structure. It can be obtained from the output file of Gaussian 16 that the total energy of the initial structure (Figure 4(a)) of 4-hydroxysalicylic acid is -2285.690 Hartree, and after geometric optimization (Figure 4(b)), the total energy of the structure is reduced to -2285.896 Hartree. Similarly, after geometric optimization, the total energy of the unit cell structure of 5-hydroxysalicylic acid decreased from -2285.674 Hartree to -2285.854 Hartree. Geometric optimization is to find the minimum point under the initial structure, and the lower the energy, the more stable the structure.

The vibration frequency was calculated using the same method and basis set on the optimized structure. The calculation of the vibration frequency in Gaussian is generally based on the harmonic oscillator model, and the corresponding harmonic potential function can be obtained only by calculating the second derivative of the energy to the coordinates. It is worth noting that the theoretically calculated spectrum is discrete actually. In order to facilitate the analysis and correspond to the experimental spectrum, the theoretical vibrational frequency spectrum is broadened. After the vibrational frequency calculation is completed, rich information can be extracted from the output file of Gaussian 16, which includes the frequency and absorbance of the spectrum. The THz-TDS system was used to measure the 4- and 5-hydroxysalicylic acid crystals to obtain their THz absorption spectra. Taking into account the influence of the system's measurement accuracy, we intercepted the spectral data within the range from 0.4-2.8 THz, and the theoretical and experimental spectra were plotted through Origin software on the same graph. The results are shown in Figure 6 and Figure 7. The matching mechanism of absorption peaks between theoretical calculations and experimental spectra is based on the principle of proximity and the position of the main peaks. Of course, if there are several absorption peaks with similar positions, the matching relationship of peak positions may

be disordered, which is the limitation of this matching mechanism. It can be seen from Figure 6, the theoretical simulation spectra of 4-hydroxysalicylic acid exhibited four distinct absorption peaks, among them at 0.61, 1.57 and 2.11 THz which respectively correspond to the absorption peaks of THz experimental spectra at 0.62, 1.63 and 1.98 THz. Meanwhile, in Figure 7, the theoretical simulation spectra of 5-hydroxysalicylic acid exhibited five distinct absorption peaks, among them at 0.69, 1.59, 2.11 and 2.64 THz which correspond to the absorption peaks of THz experimental spectra at 0.84, 1.78, 2.09 and 2.70 THz, respectively.

The number of theoretically calculated absorption peaks of 4- and 5-hydroxysalicylic acid is roughly the same as that of the experimental spectrum, and the peak positions are basically the same. At the same time, there is a certain offset between the theoretical simulation and THz experimental absorption peaks. There are many reasons for this result, such as the theoretical calculation model uses material unit cell to approximate the real crystal environment, but the results obtained in the experiment are the actual crystal samples. In addition, the harmonic approximation, functional used, basis set or the geometry obtained after optimization, which have certain influence on the accuracy in theoretical calculation. Similarly, the experiment will also be affected by other factors, such as temperature, humidity, purity and thickness of samples. Although they are the isomers, both have their own specific characteristic absorption peaks, and the numbers of

characteristic absorption peaks and the overall trend are roughly the same. In addition, the shape, intensity and positions of the absorption peaks in THz spectrum can distinguish these isomers.

Assignments of the vibrational modes

The characteristic absorption peak of the substance is closely related to the vibration mode of molecular functional groups. In order to study the cause of the characteristic absorption peak in the THz spectrum, the vibration modes of the theoretical calculation results were verified with the help of GaussView program,²⁶ and the structural vibration mode of the substance absorption peak is shown in Figure 8 and Figure 9. Meanwhile, to analyze the vibrational modes more intuitively, the normal vibration characteristics of the test sample were analyzed by PED method, and the vibration modes of each absorption peak are assigned, the results were shown in Table 1.

Figure 8 show that the vibration mode of the major absorption peaks of 4-hydroxysalicylic acid. The arrow length represents the vibration strength. And the carbon, hydrogen and oxygen atoms are colored in grey, white and red, respectively. Combined with Table 1, the vibration mode of 4-hydroxysalicylic acid at 0.61 THz is mainly the dihedral angle torsion of $C_{53}O_{54}H_{15}O_6$ atoms located in the plane. Then the vibration modes at 0.99 THz are mainly the bond angle

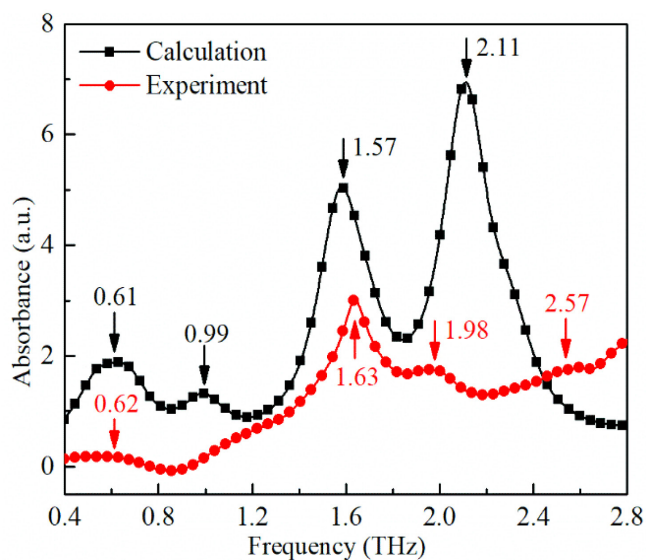


Figure 6. THz experimental and simulated spectra of 4-hydroxysalicylic acid

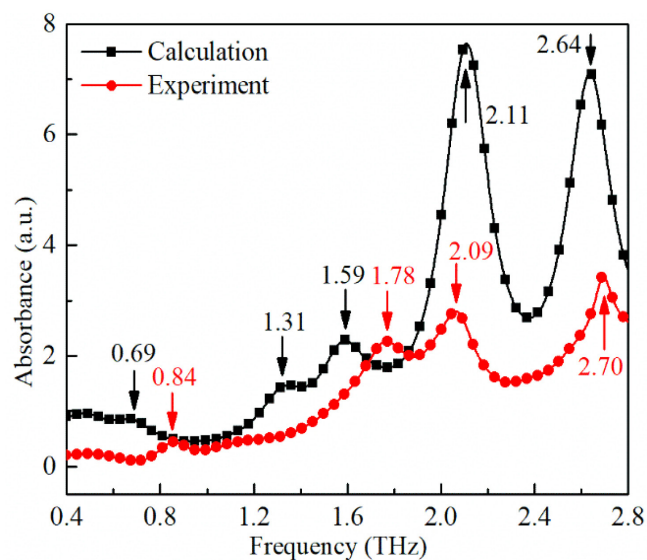


Figure 7. THz experimental and simulated spectra of 5-hydroxysalicylic acid

Table 1. Vibrational mode description assigned to each absorption peak of 4- and 5-hydroxysalicylic acid

Samples	Experiment/THz	Calculation/THz	Vibrational modes
4-hydroxysalicylic acid	0.62	0.61	T:COHO(39)
	-	0.99	B:OHO(25); T:CCCO(11)
	1.63	1.57	T:HOCC(13)
	1.98	2.11	T:HOCC(-10); T:HOCC(-14); O:CCOC(13)
	2.57	-	-
5-hydroxysalicylic acid	0.84	0.69	T:OHOC(19)
	-	1.31	B:HOC(-54)
	1.78	1.59	T:HOCC(-13); T:COHO(-17)
	2.09	2.11	T:HOCC(-11)
	2.70	2.64	T:CCCO(52)

Notes: S: Bond Length stretching; B: bond angle bending; T: dihedral angle torsion; O: the angle between the vector and the plane. The values in parentheses represent the contribution of vibration modes, and a negative sign represents the opposite vibration phase.

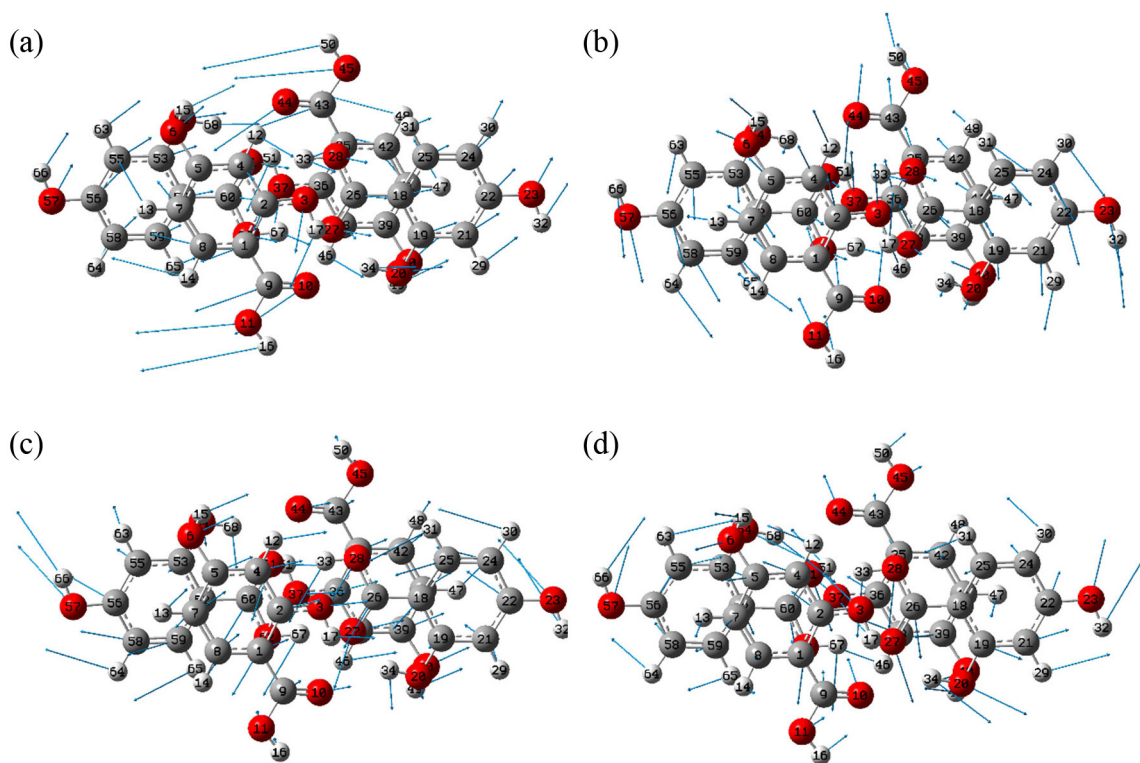


Figure 8. Vibrational modes of 4-hydroxysalicylic acid at (a) 0.61 THz, (b) 0.99 THz, (c) 1.57 THz, and (d) 2.11 THz, the arrow indicates the displacement vectors

bending involved $O_{20}H_{49}O_{40}$ atoms and the dihedral angle torsion of $C_{25}C_{18}C_{26}O_{27}$ atoms located in the plane. And the vibration modes at 1.57 THz are mainly the dihedral angle torsion of $H_{15}O_{54}C_{53}C_{52}$ atoms located in the plane. While the vibration mode at 2.11 THz is mainly the dihedral angle torsion of $H_{15}O_{54}C_{53}C_{52}$ and $H_{49}O_{40}C_{39}C_{38}$ atoms located in the plane and the angle variation between C_7C_4 vector and $C_4O_6C_5$ affiliated plane.

Figure 9 show that the vibration mode of the major absorption peaks of 5-hydroxysalicylic acid. Combined with Table 1, the vibration mode of 5-hydroxysalicylic acid at 0.69 THz is mainly the dihedral angle torsion of $O_{43}H_{49}O_{10}C_2$ atoms located in the plane. Then the vibration modes at 1.31 THz are mainly the bond angle bending involved $H_{17}O_{27}C_{19}$ atoms. While the vibration modes at 1.59 THz are mainly the dihedral angle torsion of $H_{17}O_{27}C_{19}C_{18}$ and $C_{19}O_{27}H_{17}O_{11}$

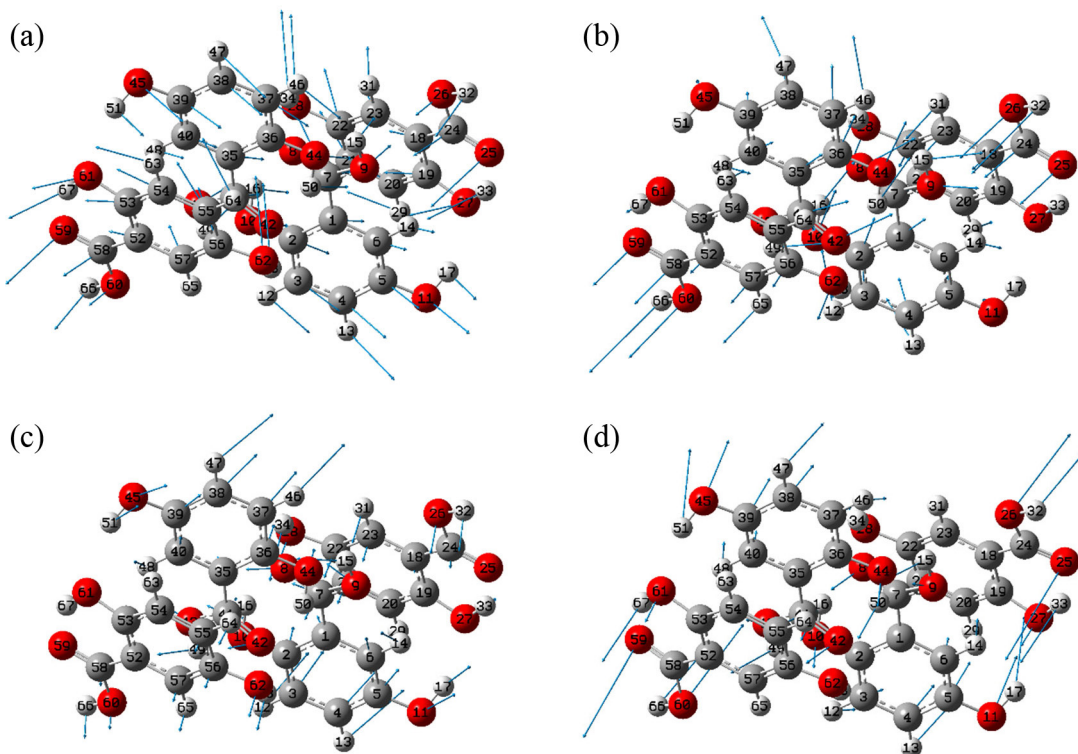


Figure 9. Vibrational modes of 5-hydroxysalicylic acid at (a) 1.31 THz, (b) 1.59 THz, (c) 2.11 THz, and (d) 2.64 THz, the arrow indicates the displacement vectors

atoms located in the plane. And the vibration mode at 2.11 THz is mainly the dihedral angle torsion of $H_{17}O_{11}C_5C_4$ atoms located in the plane as well as the vibration mode at 2.64 THz prevailing due to the dihedral angle torsion of $C_{33}C_{52}C_{58}O_{60}$ atoms located in the plane.

According to the above analysis, the characteristic absorption peaks of 4- and 5-hydroxysalicylic acid in the 0.4 to 2.8 THz region are caused by the normal vibration of the molecular groups. PED analysis results show the absorption peaks of 4- and 5-hydroxysalicylic acid are mainly derived from the vibration mode of dihedral angle torsion. The source of the characteristic absorption peak can be attributed to the vibration mode of the molecular groups, and the nature of the molecular groups vibration mode can be attributed to the molecules interaction.

Visual analysis of chemical bond and weak interaction

In order to further analyze the formation mechanism of 4- and 5-hydroxysalicylic acid spectral absorption peaks in the THz frequency band, the IRI method was used to investigate the chemical bonds and weak interactions in the system. This method can be implemented in the wave function analysis program Multiwfn.²⁷ Simultaneously, through VMD and Gnuplot software, iso-surface maps and scatter plots can be drawn. The results are shown in Figure 10 and Figure 11. Among them, carbon, hydrogen and oxygen atoms are represented by cyan, white and red respectively. Figure 10(b) and Figure 11(b) include chemical bonds and weak interaction regions. While in Figure 10(c) and Figure 11(c), the scale value of $\text{sign}(\lambda_2)\rho$ ranges from -0.06 to +0.06, and this area is mainly composed of weak interactions. It can be seen from Figure 10(a) that there is a large area of green iso-surface in the 4-hydroxysalicylic acid system structure. Combined with the color scale diagram of chemical bonds and weak interactions described in Figure 3, the green iso-surface represents Van der Waals effect, which indicates that the intermolecular interactions in 4-hydroxysalicylic acid are dominated in quantity by van der Waals interactions. van der Waals interactions can effectively cancel themselves out, and they are significantly weaker than the hydrogen bonds, so van der Waals

interactions may be the most abundant, but not necessarily the most important or the dominant ones. In addition, the positions of intra- and inter-molecular O-H...O are blue iso-surfaces, and the positions of intra- and intermolecular C-H...O are the green and brown iso-surfaces, which can be regarded as hydrogen bonds. The middle position of the benzene ring shows red, which can be regarded as a steric effect. And the blue iso-surfaces between C-C, C-O and C-H can be regarded as the chemical bonds. In Figure 10(b), the value of $\text{sign}(\lambda_2)\rho$ has multiple blue spikes in the range of -0.4 to -0.28, corresponding to the chemical bonds of C-C, C-O and C-H, and negative values indicate attraction. In Figure 10(c), the area where the value of $\text{sign}(\lambda_2)\rho$ is close to zero indicates the van der Waals effect, and the points in this area are denser, further confirming that the intermolecular interaction is mainly dominated in quantity by the van der Waals effect. There are multiple blue spikes where the value of $\text{sign}(\lambda_2)\rho$ is in the range of -0.05 to -0.04, which correspond to intra- and inter-molecular O-H...O hydrogen bonds. There are green and brown spikes where the value of $\text{sign}(\lambda_2)\rho$ near -0.012 and +0.012 respectively, corresponding to intra- and inter-molecular C-H...O hydrogen bonds, in which the green position is attractive and the brown position is repulsive. There are red spikes where the value of $\text{sign}(\lambda_2)\rho$ is in the range greater than +0.018, which corresponds to the steric hindrance in the benzene ring of the molecular structure.

As shown in Figure 11(a), there is a large area of green iso-surface in the molecular system structure, indicating that the intermolecular weak interactions in 5-hydroxysalicylic acid are dominated in quantity by van der Waals interactions. It is clear that the chemical bonds and weak interactions of the molecular systems in 4- and 5-hydroxysalicylic acid are roughly the same comparing Figure 10 and Figure 11. This is because they are isomers and the structure is basically the same. At the same time, there are differences between them. As shown in Figure 10(c), there are three blue spikes that the value of $\text{sign}(\lambda_2)\rho$ is in the range of -0.05 and -0.04, corresponding to O-H...O hydrogen bonds. And the spikes correspond to the C-H...O hydrogen bonds where the value of $\text{sign}(\lambda_2)\rho$ near -0.012. While in Figure 11(c), there are two blue spikes that the value of $\text{sign}(\lambda_2)\rho$ near -0.04 under the same O..H-O hydrogen bonds. While the value of

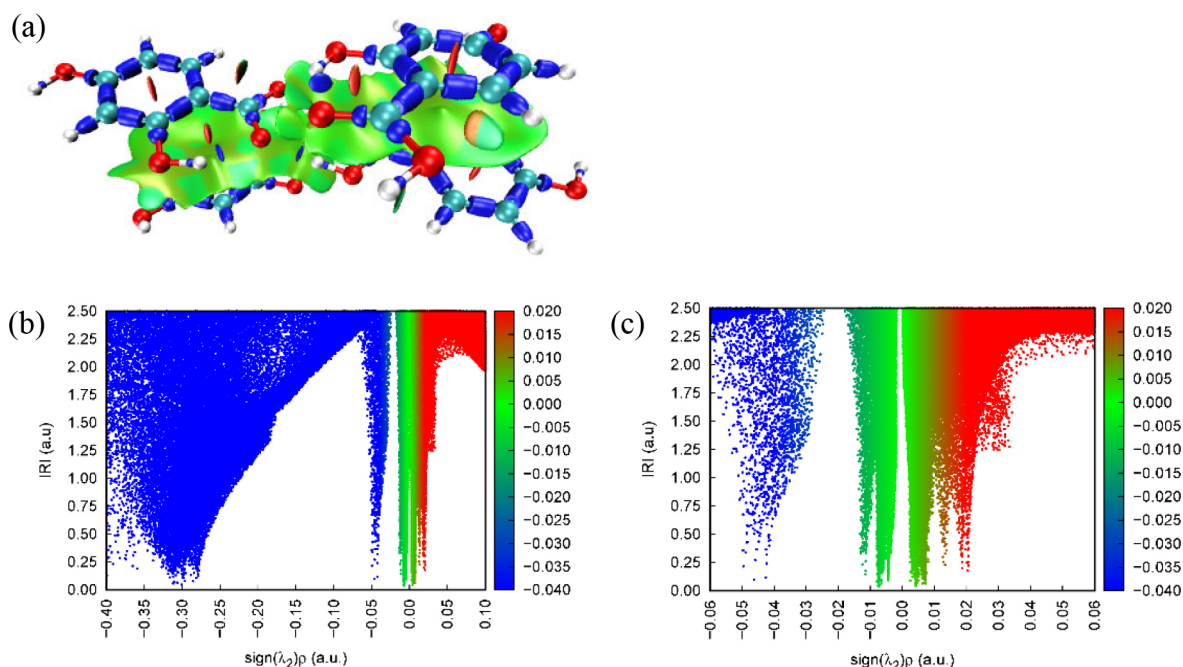


Figure 10. IRI analysis results of 4-hydroxysalicylic acid. (a) three-dimensional isosurfaces. (b) two-dimensional scatter plots, $\text{sign}(\lambda_2)\rho$ from -0.4 to +0.1. (c) two-dimensional scatter plots, $\text{sign}(\lambda_2)\rho$ from -0.06 to +0.06

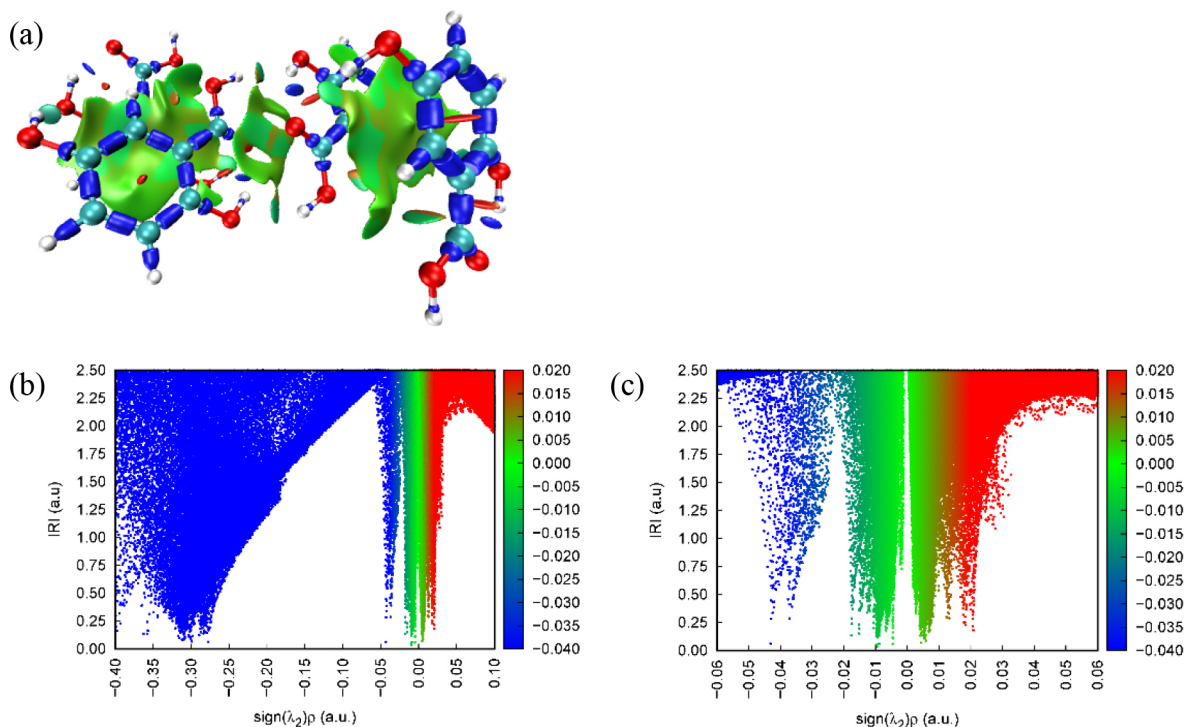


Figure 11. IRI analysis results of 5-hydroxysalicylic acid. (a) three-dimensional isosurfaces. (b) two-dimensional scatter plots, $\text{sign}(\lambda_2)\rho$ from -0.4 to +0.1. (c) two-dimensional scatter plots, $\text{sign}(\lambda_2)\rho$ from -0.06 to +0.06

$\text{sign}(\lambda_2)\rho$ is close to -0.02 under the same C-H...O hydrogen bonds, and the position of spikes corresponding to the hydrogen bond is offset. IRI analysis showed that the intermolecular weak interactions in 4- and 5-hydroxysalicylic acid were dominated in quantity by van der Waals interactions.

CONCLUSIONS

The THz spectra of 4- and 5-hydroxysalicylic acid from 0.4 to 2.8 THz at room temperature were measured by using THz-TDS. It is found that there are different characteristic absorption peaks of both, which can be used as characteristic fingerprints to detect and identify the isomers. The theoretical calculation of the substance unit cell by using DFT method, and the characteristic absorption peaks of theory and experiment are basically the same. In order to further study the mechanism of absorption spectrum, the vibrational characteristics, chemical bonds and weak interactions in molecular systems were studied by using PED and IRI method. The PED analysis confirms that the majorities of vibration modes in 4- and 5-hydroxysalicylic acid are the dihedral angle torsion. While the IRI analysis confirms that the chemical bond in 4- and 5-hydroxysalicylic acid systems are roughly the same, and intermolecular weak interaction of both are mainly dominated in quantity by van der Waals interaction. In conclusion, this is a novel and effective way to identify isomers by using THz-TDS technology. More importantly, it provides a valuable analytical method or reference for understanding the characteristics of terahertz spectrum by combining PED and IRI methods.

ACKNOWLEDGEMENTS

This work is funded by the National Natural Science Foundation of China under Grant No.62063003, and is partly supported by National Natural Science Foundation of China under Grant No.62161005, and is partly supported by the Guangxi Key Research and Development Plan under Grant No.2020AB44003, and is partly

supported by the Guangxi Key Laboratory of Automatic Detecting Technology and Instruments under Grant No. YQ19102.

REFERENCES

- Balakrishna, M.; Rao, G. S.; Ramanaiah, M.; *Res. J. Pharm. Technol.* **2017**, *10*, 3681 [Crossref].
- Witko, E. M.; Buchanan, W. D.; Korter, T. M.; *J. Phys. Chem. A* **2011**, *115*, 12410 [Crossref].
- Hermet, P.; Bantignies, J. L.; Maurin, D.; *Chem. Phys. Lett.* **2007**, *445*, 47 [Crossref].
- Yan, F.; Li, W.; Wang, Z. C.; *Spectrosc. Spectral Anal.* **2020**, *40*, 397 [Crossref].
- Sun, J. H.; Shen, J. L.; Liang, L. S.; *Chin. Phys. Lett.* **2005**, *22*, 3176 [Crossref].
- Wang, P.; He, M. X.; Li, M.; *Spectrosc. Spectral Anal.* **2020**, *40*, 6.
- Yamaguchi, M.; Miyamaru, F.; Yamamoto, K.; *Appl. Phys. Lett.* **2005**, *86*, 3625 [Crossref].
- Zheng, Z. P.; Fan, W. H.; Hui, Y.; *Chem. Phys. Lett.* **2012**, *525*, 140 [Crossref].
- Ding, L.; Fan, W. H.; Song, C.; *J. Appl. Spectrosc.* **2019**, *85*, 1 [Crossref].
- Saito, S.; Inerbaev, T. M.; Mizuseki, H.; *Jpn. J. Appl. Phys.* **2006**, *45*, 4170 [Crossref].
- Takahashi, M.; Ishikawa, Y.; Ito, H.; *Chem. Phys. Lett.* **2012**, *531*, 98 [Crossref].
- Chen, T.; Li, Z.; Yin, X. H.; *Spectrochim. Acta, Part A* **2016**, *153*, 586 [Crossref].
- Chen, T.; Li, Z.; Hu, F. R.; *Spectrosc. Spectral Anal.* **2017**, *37*, 618.
- Wang, Y.; Zhao, Z.; Chen, Z.; *J. Appl. Phys.* **2007**, *102*, 22 [Crossref].
- Duvillaret, L.; Garet, F.; Coutaz, J. L.; *IEEE J. Sel. Top. Quantum Electron.* **2002**, *2*, 739 [Crossref].
- Dorney, T. D.; Baraniuk, R. G.; Mittleman, D. M.; *J. Opt. Soc. Am. A* **2001**, *18*, 1562 [Crossref].
- Hua, Y.; Zhang, H.; Zhou, H.; *IEEE Trans. Instrum. Meas.* **2010**, *59*, 1414 [Crossref].

18. Nityananda, R.; Hohenberg, P.; Kohn, W.; *Resonance* **2017**, *22*, 809 [Crossref].
19. Groom, C. R.; Bruno, I. J.; Lightfoot, M. P.; *Acta Crystallogr., Sect. B: Struct. Sci., Cryst. Eng. Mater.* **2016**, *72*, 171 [Crossref].
20. Grimme, S.; Antony, J.; Ehrlich, S.; *J. Chem. Phys.* **2010**, *132*, 154104 [Crossref].
21. Wang, Q.; Xue, J.; Wang, Y.; *Spectrochim. Acta, Part A* **2018**, *204*, 99 [Crossref].
22. Jens, N.; Heinrich, N.; Schmuttenmaer, C. A.; *J. Phys. Chem. A* **2018**, *122*, 5978 [Crossref].
23. Jamróz, M. H.; *Spectrochim. Acta, Part A* **2013**, *114*, 220 [Crossref].
24. Lu, T.; Chen, Q. X.; *Chemistry – Methods* **2021**, *1*, 231 [Crossref].
25. Johnson, E. R.; Keinan, S. P.; Mori-Sanchez, P.; Contreras-García, J.; Cohen, A. J.; Yang, W.; *J. Am. Chem. Soc.* **2010**, *132*, 6498 [Crossref].
26. Liu, X. D.; Hu, Z. Q.; *College Chemistry* **2006**, *5*, 34 [Crossref].
27. Lu, T.; Chen, F.; *J. Comput. Chem.* **2012**, *33*, 580 [Crossref].